DYNAMIC PERFORMANCE OF FLETTNER ROTORS WITH AND WITHOUT THOM DISCS

T. J. Craft, H. Iacovides and B. E. Launder
Turbulence Mechanics Group, School of MACE
University of Manchester, Manchester, UK.
brian.launder@manchester.ac.uk

ABSTRACT

The paper presents U-RANS simulations for 3-dimensional flow past a rotating cylinder for a range of Reynolds numbers and rotation rates relevant to the performance of ships propelled by Flettner rotors in place of sails. Comparisons are first drawn with existing LES data of similar flows at much lower Reynolds numbers. Thereafter the performance is examined for values of Re within the probable range of actual rotor operating conditions, including an exploration of the effect of adding discs mounted along the length of the cylinder which Thom (1934) had suggested led to improved performance at high spin rates.

INTRODUCTION

In the early Twenties collaborative work by Prandtl (1925) and Anton Flettner led to the conclusion that the Magnus effect[1] could be exploited to provide an efficient and effective way of propelling ships. In demonstration, Flettner replaced the sails on two barquentine ships, by twin vertical rotors. One of the ships, originally the ***Buckau*** but re-named, following conversion, the ***Baden Baden*** thereafter crossed the Atlantic, Fig. 1. The rotors, which became immediately known as ***Flettner rotors***, had numerous advantages over conventional wind-driven propulsion, being only one quarter of the weight of the masts, sails and rigging they replaced and permitting the vessel to make more rapid progress over a wide range of wind speeds and directions than conventional sails. Further commercial development did not take place, however, due to the grave financial depression of the late 1920's and to the emergence of diesel-powered craft (and the plentiful supply and consequent low price of diesel fuel).

Now, in the 21st Century, with fuel prices having soared and a growing recognition of the necessity to slash CO_2 emissions urgently, the potential of the Flettner rotor is again being seriously examined. Enercon, the wind-turbine company, has commissioned and brought into service in late 2010 a vessel for delivering the shafts and rotors of its turbines that has four Flettner rotors as its primary source of propulsion. Even more ambitious (Salter et al., 2008) is a proposal to build a fleet of 1500 unmanned, radio-controlled craft driven by Flettner rotors. These would eject vertically a fine mist of seawater and, on the evaporation of the water, would leave ultra-fine salt grains, a proportion of which would be lofted to form additional cloud condensation nuclei thus brightening the low-level marine stratus clouds to reflect an increased proportion of incident sunlight. The above authors believe that such a fleet would be sufficient to reduce the sunlight incident upon the earth by roughly 2% which should reduce global mean temperatures to those prevailing at the start of the industrial revolution. In fact, Salter et al. (2008) proposed that discs should be added along the length of the spinning cylinders since Thom (1934) had reported that this modification significantly increased the attainable lift coefficient for normalised rotor-spin velocities, $\Omega \equiv U_{spin}/U_{wind}$, greater than 4. Further experiments with a bare rotor have been reported by Reid (1924) with a view to possible use on aircraft and by Bergeson & Greenwald (1985) for a rotor mounted on a test vessel.

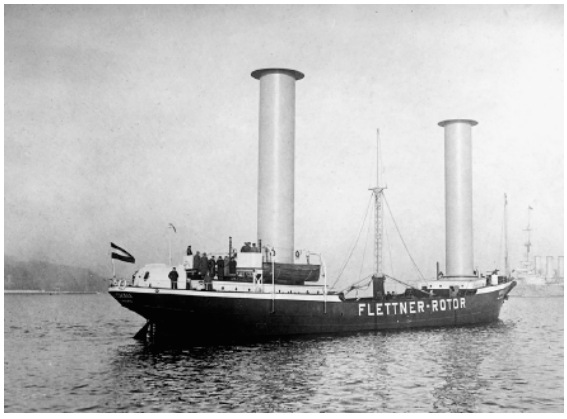

Figure 1. Photograph of the original Flettner rotor ship.

More than 75 years on from Thom's experiments, computational studies of the spinning cylinder seem the most productive route to explore aerodynamic aspects relating to the performance of Flettner rotors with or without discs. There have been several impressive studies of two-dimensional flow around a smooth cylinder for laminar flow up to Reynolds numbers of a few hundred and Ω as high as 12 (Stojkovic et

[1] in which a spinning cylinder past which an external stream is flowing receives a lateral thrust due to the lower pressure on the side of the cylinder where the cylinder's motion is in the same direction as the streaming flow.

al., 2002; Mittal & Kumar, 2003; Padrino & Joseph, 2006; El Akoury et al., 2009). These have shown that for normalized spin rates much in excess of 2 the conventional Karman vortex is suppressed, the lift coefficient rises strongly with spin rate but that large amplitude pulsations on the rotor occur over a narrow range of rotation rates for Ω between 3.5 and 5.5, the precise range depending upon Reynolds number, El Akoury et al. (2009). These last authors also looked at 3D simulations but apparently only for Ω up to 0.5. Very recently Karabelas (2010) has reported an LES study at Re = 140,000 (which we note is still many times less than that at which sea-going Flettner-rotor vessels would operate). That study found no such periodicities in drag or lift (once the spin ratio was high enough to suppress the conventional Karman vortex) but the maximum value of Ω was only 2.0 so this result was not in conflict with the previous laminar studies at lower Re.

In a previous publication, using an unsteady RANS strategy, the present authors (see Latham et al., 2011) have found that for a Reynolds number of $8x10^5$ no periodic forcing occurred for Ω equal to 3.0 and 5.0. There were, however, small irregular variations associated with temporal variations in the shed vortices. The addition of discs brought no overall enhancement of lift coefficient, but they did remove the slight temporal irregularity noted above for the smooth cylinder.

The above results left a number of questions unresolved some of which the present paper has endeavoured to answer. The first is whether the instabilities noted in the 2D laminar flow results also appeared in turbulent flow. The second issue is the apparently contradictory findings of Thom's experiments and the authors' earlier CFD results of the effectiveness of Thom discs. Comparisons are also drawn with the bare cylinder LES study of Karabelas (2010) to assess the likely adequacy of the closure modelling included within the present U-RANS computations. The sections below first summarize the computational and turbulence models applied, before presenting the current results and finally drawing conclusions.

NUMERICAL MODEL

Three-dimensional, time-dependent computations have been carried out with the in-house flow solver STREAM. It is a finite-volume, general-geometry code with a collocated grid, using Cartesian velocity decomposition. The pressure is obtained through the SIMPLE algorithm. The bounded high-order UMIST scheme, Lien and Leschziner (1994), is used for the discretisation of convection and the Crank-Nicolson scheme for temporal discretisation. Two versions of this code have been employed, one using a single block and one employing a multi-block grid. In the single block version, the rotating cylinder is placed at the centre of a cylindrical polar mesh extending to a radius 10 times that of the cylinder. The multi-block arrangement allows for a solution domain which downstream of the cylinder has a rectangular shape and it is longer than the upstream section. In both approaches a fixed cross-flow velocity is specified along the upstream boundary, with zero-gradient (in the main flow direction) conditions along the exit boundaries. Either symmetry or repeating flow boundary conditions were imposed in the axial direction. Here the computations presented have been produced by the multi-block version, shown in Fig. 2, with grids containing up to 0.9 million cells, and non-dimensional time steps of around $0.01U/R$ (U being the free-stream velocity and R the cylinder radius), sufficiently small to ensure there were at least 600 time steps covering a typical vortex shedding cycle from the cylinder.

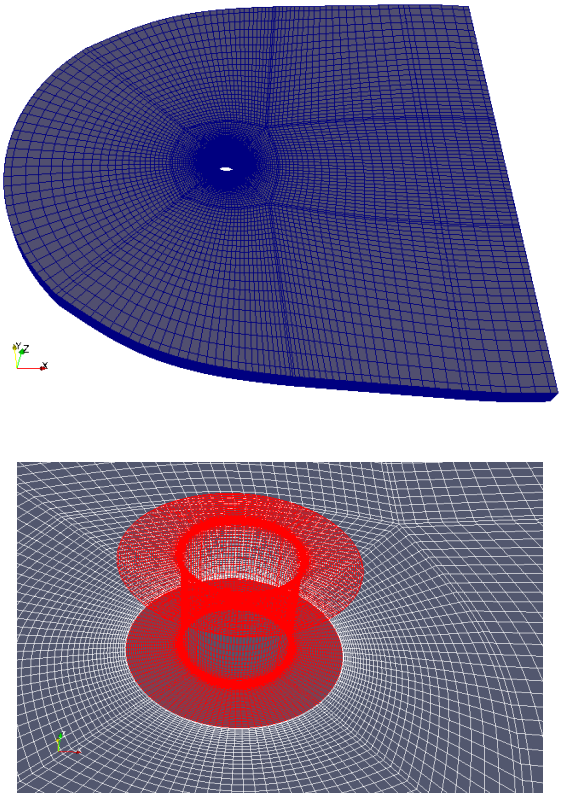

Figure 2. Overall view and detail of the non-orthogonal grid

TURBULENCE MODEL

At the high Reynolds numbers at which Flettner rotors operate, it is impractical to resolve in detail the near-wall viscosity-affected sub-layer[2]. In the results presented here the standard log-law based wall-function of Chieng & Launder (1980) has thus been used to cover this region on both the cylinder and disc surfaces.

Despite the computational convenience of conventional wall-functions such as the above, they are known to be rather

[2] Although for a small section of a single rotor a fine-grid "low-Reynolds-number" treatment would be feasible that would not be the case for a complete rotor still less for several rotors mounted close together.

unreliable in capturing features such as significant streamwise pressure gradients, or the considerable skewing that is likely to occur across the very near-wall region, particularly when Thom discs are added. Future calculations may, therefore, test the effect of employing more advanced wall-functions such as the Analytical Wall-Function (AWF) approach, described in Craft et al. (2002) and more recently extended to three-dimensional flow where the velocity vector parallel to the wall undergoes considerable skewing across the viscosity-affected sublayer (Zacharos, 2010; Craft et al., 2008).

The sublayer treatment above, which is applied to a thin region close to all rigid surfaces, can be matched to any desired turbulence model for the remainder of the flow. The majority of the present results have been obtained with a form of k-ε linear eddy-viscosity model containing a near-wall length-scale control to prevent excessive length scales arising in adverse-pressure-gradient regions (Yap, 1987), although in the present computations with a wall-function applied at the near-wall node this term is unlikely to have a particularly large effect on the solution.

Further results have been obtained with the two-component-limit (TCL) stress-transport closure[3] of Craft et al. (1996), the most advanced RANS model used by our group, that has been successfully applied to a wide range of challenging 3D turbulent flows near walls (e.g. Craft & Launder, 2001). This model overall clearly outperforms eddy-viscosity models (EVMs), though for the present cases, within a U-RANS solver where the resulting unsteadiness may contribute a major proportion of the momentum transport, the differences are relatively small. Consequently, because of the lower computational and core demands, most results have been obtained with the simpler EVM.

PRESENTATION AND DISCUSSION OF RESULTS

The first computations were made in 2D mode at Reynolds numbers below 500 to verify that the present simulations accorded closely with those reported earlier by those examining laminar flows. Particular attention was given to the study of Mittal & Kumar (2003) at Re=200. Virtually complete agreement with the effects of increasing the spin ratio were found: the suppression of the Karman vortex shedding at Ω=3.0, the appearance of large amplitude fluctuations for Ω=4.4 and their disappearance by Ω=5.0 giving a lift coefficient C_L in excess of 25. These have been reported in detail in Craft et al. (2010) and are not re-presented here.

Next, in 3D mode, attention has been given to the cases at Re = 1.4×10^5 examined via LES by Karabelas (2010), shown in Figs. 3-5. The modification of the time-averaged streakline pattern around the cylinder (from the symmetric pattern for Ω=0, not shown) for Ω=1 and 2 is evident in Fig. 3 where the

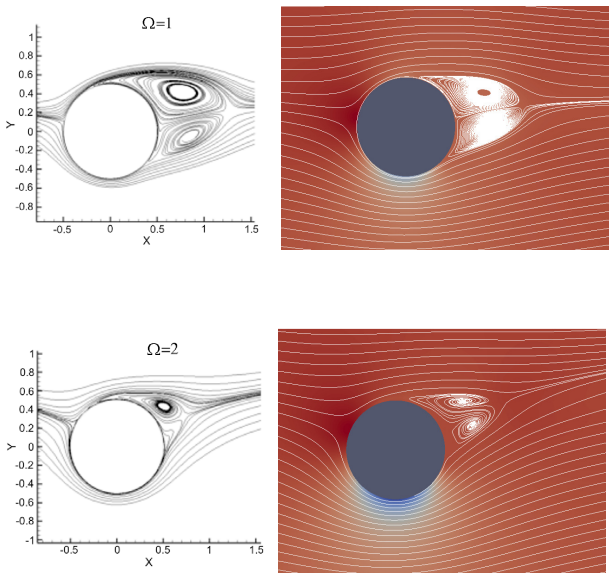

Figure 3. Comparison of mean streaklines created by flow past a spinning cylinder. Left: LES data of Karabelas; Right: Present U-RANS. Top Ω=1; Bottom Ω=2.

cylinder spins anticlockwise. At the lower spin rate two separated flow zones are still present, though clearly distorted by the cylinder rotation. At the higher spin rate the accord between the LES and the TCL U-RANS results is still broadly satisfactory though the lower of the separation zones, that the LES data suggest is entirely suppressed, is still evident for the U-RANS computation. The progressive modification in flow pattern shown in Fig. 3 leads to an increase in lift coefficient with spin ratio shown in Fig. 4a. The overall behaviour is reproduced slightly better with the TCL model than the k-ε EVM though the latter better captures the LES level of lift at the highest spin rate. The TCL scheme also captures the drag coefficient more closely, Fig. 4b, though neither model is particularly close at Ω=1. The reason for this can be inferred from Fig. 5 which shows the pressure variation around the cylinder. Evidently, for 135°<θ<270° (covering most of the downwind face of the cylinder) the static pressure is higher than for the LES data resulting in a lower drag coefficient. For no rotation, separation occurs earlier with the TCL model than with the EVM and this accords well with the LES behaviour. It is noted, in passing, that the experimental data at Re=6×10^4 of Aoki & Ito (2001) shows rather closer agreement to TCL drag coefficients than do the LES data. At the highest spin rate, however, the EVM computations reproduce the more rapid fall in pressure from 0-90° indicated by the LES data and this is crucial to the superior lift coefficient at this spin ratio seen in Fig. 4a.

A comparison over a wider range of spin ratios and Re appears in Figs. 6 and 7. Included in the figures are the early data of Reid (1924) and the Bergeson & Greenwald (1985)

[3] A model which incorporates constraints so that, as the wall is approached, turbulent fluctuations normal to the wall vanish faster than wall-parallel components (as required by continuity). Thus, in the limit the modelled turbulent stresses reach the two-component limit.

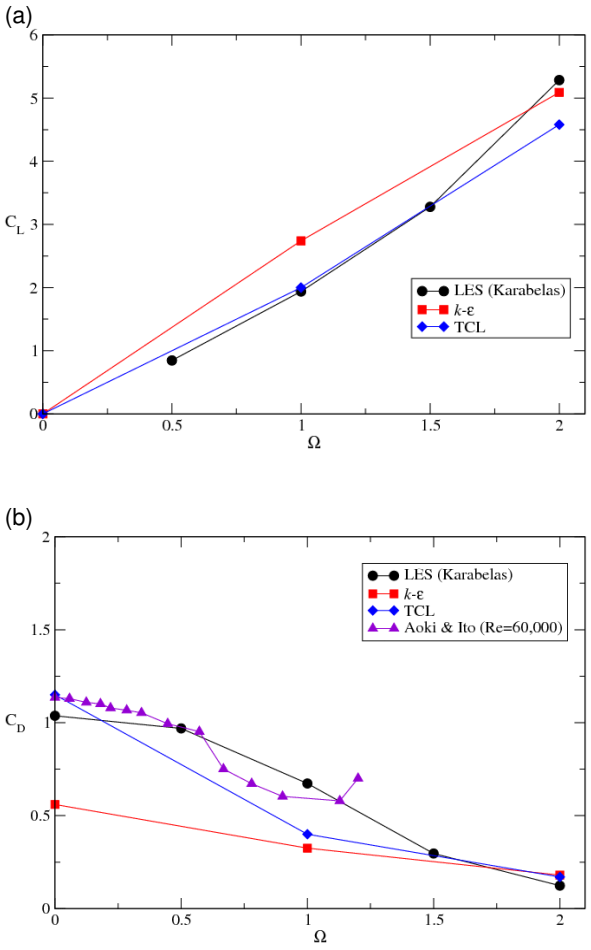

Figure 4. Predicted mean lift (a) and drag (b) coefficients for rotating cylinder at Re=1.4x10^5, compared with the LES data of Karabelas (2010).

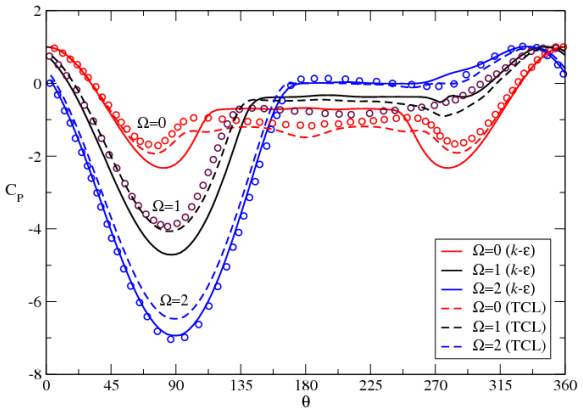

Figure 5. Predicted pressure coefficients around rotating and non-rotating cylinder at Re=1.4x10^5, compared to the LES data of Karabelas (2010).

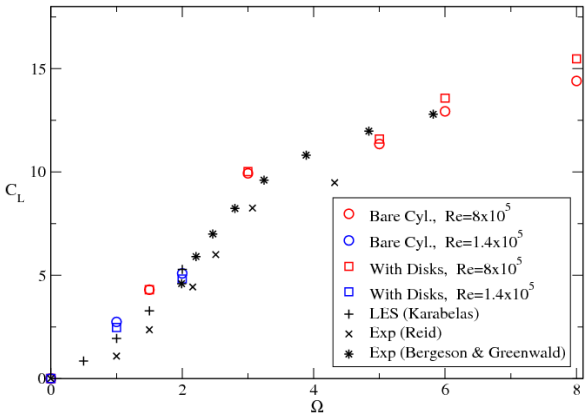

Figure 6. Predicted and measured mean lift coefficients for rotating cylinders with and without Thom discs.

data. There is generally good accord among the lift coefficients reported from different sources which exhibit initially a virtually linear growth in C_L with Ω but then, for spin ratios greater than 3, a more gradual rise. This pattern is well captured by the U-RANS computations (obtained with the EVM). There is, however, a striking difference in the drag coefficient, Fig. 7, where the Reid data, after initially falling with Ω, show a marked rise. Bergeson & Greenwald (1985) do not report C_D variations but the U-RANS computations are, as noted above, in reasonable agreement with the Karabelas (2010) LES data. At the high Reynolds numbers here considered the main contribution to the drag is associated with the imbalance of static pressure on the upstream and downstream faces of the cylinder rather than wall friction. The fact that the Reid data of C_L are slightly lower than the other data while C_D are higher perhaps suggests a relatively small error in determining the angular orientation.

Finally, the effect of adding discs in the manner of Thom is considered. Only a single geometric arrangement has been examined. The axial spacing, h, between adjacent discs equals the cylinder diameter, d, while the discs themselves are of diameter 2d. Spinning discs are known to generate locally a complex flow field with a centrifugally-driven radial outflow adjacent to the disc (the Ekman layer). It is thus hard to foresee what effect the interaction of this flow with the apparent wind will have on the distribution of static pressure around the cylinder (which, of course, largely determines the lift and drag coefficients). The computed values of these parameters for the case with discs is also included in Figs. 6 and 7. At low rotation speeds there is scarcely any difference in lift coefficient while the drag coefficient for the case with discs is slightly greater than for the bare cylinder. However, for spin ratios of 5 and above the drag falls to or below that for the bare cylinder while the lift increases with Ω rather faster

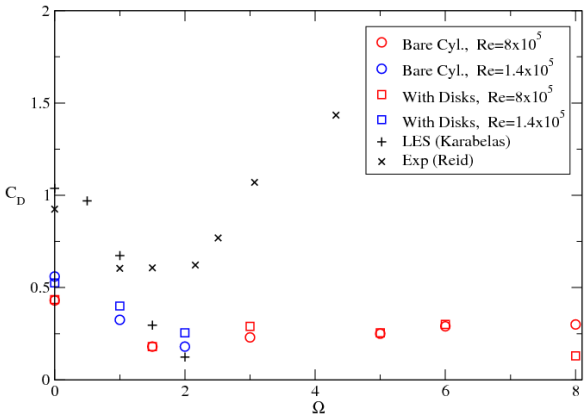

Figure 7. Predicted and measured mean drag coefficients for rotating cylinders with and without Thom discs.

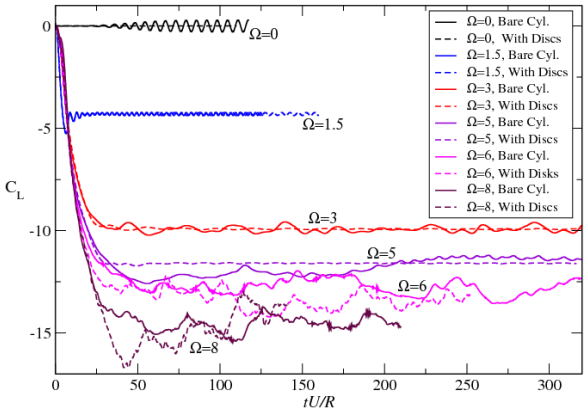

Figure 8. Predicted lift-coefficient histories for rotating cylinders with and without Thom discs.

than for the bare cylinder. Indeed, for Ω=8 the lift coefficient is 8% greater while the drag is less than half that for a bare cylinder. The detailed role of the discs on the flow dynamics requires deeper investigation than we have so far been able to provide. On the one hand, Fig. 8 shows that for moderate spin rates (Ω=3 or 5) the discs smooth out the temporal unsteadiness in lift (and drag, not shown). For Ω=5, Fig. 9 provides a snapshot of the flow around the cylinder for the two cases, i.e. with and without discs, using the Q-Criterion to distinguish the flow patterns. Without discs the flow is strongly unsteady while, with the discs added, the flow in the vicinity of the cylinder is invariant with time with just a mild temporal fluctuation visible in the tails of the horseshoe vortices created on the upstream side by the disc-cylinder intersections. However, as Fig. 8 makes clear, at higher spin rates, the discs fail to cause any significant suppression of the fluctuations.

Finally, it is noted that the boundary conditions applied at the upper and lower ends of the domain ($z=h$ and 0) can have a significant effect on the results in the case where discs are present. Most of the computations have been run assuming (as remarked earlier) periodic boundary conditions on these planes. However, for Ω=6, tests were also made with symmetry boundary conditions applied instead. For the bare cylinder the two runs lead to sensibly the same randomly fluctuating behaviour. When discs are present, however, the application of symmetry boundary conditions (for radii greater than that of the discs) entirely suppresses the fluctuations. For an actual multi-disc rotor neither boundary condition is correct. Indeed, the only sure route is to include the whole rotor within the computation because clearly (just above the top of the rotor) the free passage of the wind and (beneath the lower end of the rotor) the deck and superstructure will each have an effect on the rotor dynamics.

CONCLUSIONS

The paper has reported U-RANS computations of the flow past a section of a spinning rotor with a view to comparing results with earlier studies at low Reynolds number and, principally, to assessing the likely performance of a Flettner rotor over a range of conditions. First, regarding laminar flow, it is noted that our earlier 2-dimensional simulations have confirmed the large-amplitude, low-frequency periodicities previously reported by others over a narrow range of rotation rates.

In turbulent flow, no such large amplitude periodicities have been found, however. Close agreement has been obtained with the LES lift and drag coefficients of Karabelas (2010) which is encouraging since the cost of a U-RANS computation is at least an order of magnitude less than for LES. Turning to the rotor performance at the high Reynolds numbers encountered in actual Flettner rotors, for a bare cylinder very satisfactory accord with the lift coefficients reported in two sets of experimental data for spin ratios up to 6 has been obtained. The effect of adding discs at intervals along the spinning cylinder as advocated by Thom (1934) led, at low spin rates, to negligible change in lift coefficient and modestly higher drag coefficient. For spin ratios above 5, however, the lift coefficient is higher by up to 10%. However, this is a markedly smaller improvement than reported by Thom, but the discs in his experiments were of larger diameter relative to the cylinder and with closer spacing, which may possibly account for the greater augmentation of lift.

While the present U-RANS study has found encouraging agreement with the available experimental and LES data, it would be desirable, before embarking on an examination of further practical issues and fundamental aspects of Flettner-rotor performance, to embed a more generally applicable wall treatment (such as the AWF scheme that allows vector skewing within the viscous sublayer and an effective sublayer thickness sensitive to locally prevailing conditions, Craft et al., 2008) in place of the relatively rudimentary wall functions currently adopted.

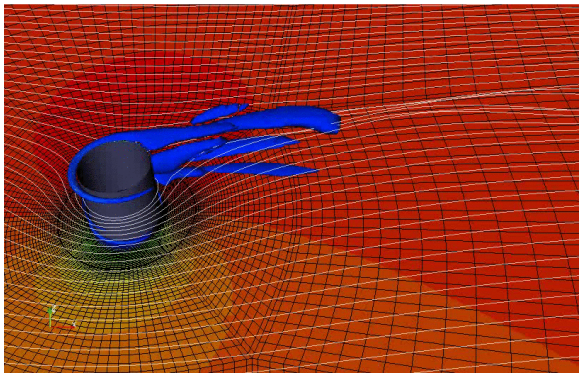

Bare Cylinder

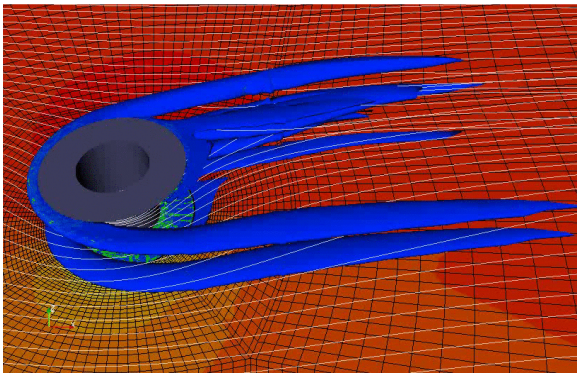

Cylinder with Thom Discs

Figure 9. Instantaneous snapshot of Q-criterion isosurface for flow around a cylinder with and without Thom discs at Ω=5; Re=8x10^5.

REFERENCES

Aoki, K. and Ito, T., 2001, Flow characteristics around a rotating cylinder, *Proc. School of Eng'ng, Tokai Univ*., **26**, 29-34.

Bergeson, L. and Greenwald, C. K., 1985, Sail assist developments 1979-85, *J. Wind Eng'ng & Indust. Aerodyn*., **19**, 45-114.

Chieng, C. C. and Launder, B. E., 1980, On the calculation of turbulent heat transfer downstream from an abrupt pipe expansion, *Numerical Heat Transfer*, **3**, 189-207.

Craft, T. J., Gerasimov, A. V., Iacovides, H. and Launder, B. E., 2002, Progress in the generalization of wall-function treatments, *Int. J. Heat & Fluid Flow*, **23**, 148-160.

Craft, T. J., Iacovides, H. and Launder, B. E., 2010, Computational modelling of Flettner-rotor performance with and without Thom discs, *Proc. 7th Conf. on Eng'g Turbulence Modelling & Meas.*, Marseilles.

Craft, T. J., Iacovides, H., Launder, B. E. and Zacharos, A., 2008, Some swirling-flow challenges for turbulent flow CFD, *Flow Turbulence & Combustion,* **80,** 419-434.

Craft, T. J., Ince, N. Z., and Launder, B. E., 1996, Recent developments in second-moment closure for buoyancy-affected flows, *Dynamics of Atmospheres and Oceans*, **23**, 99-114.

Craft, T. J. and Launder, B. E., 2001, Principles and performance of TCL-based second-moment closures, *Flow Turbulence & Combustion*, **66**, 253-272.

El Akoury, R., Martinat, G., Braza, M., Perrin, R., Hoarau, Y., Harran, G. and Ruiz, D., 2009, Successive steps of 2D and 3D transition in the flow past a rotating cylinder at moderate Reynolds numbers, in *IUTAM Symp on Unsteady Separated Flows & their Control* (M. Braza & K. Hourigan, Eds), IUTAM Book Series 14, Springer.

Karabelas, S. J., 2010, Large-eddy simulation of turbulent flow past a rotating cylinder, *Int J. Heat & Fluid Flow*, **31**, 518-527.

Latham, J., et al., 2011, Marine cloud brightening, *Phil Trans Roy. Soc.* (To appear).

Lien, F-S. and Leschziner, M. A., 1994, Upstream monotonic interpolation for scalar transport with application to complex turbulent flows, *Int. J. Num. Meth. in Fluids*, **19**, 527–548.

Mittal, S. and Kumar, B., 2003, Flow past a rotating cylinder, *J. Fluid Mech*., **476**, 303-334.

Padrino, J. C. and Joseph, D. D., 2006, Flow past a rotating cylinder, *J. Fluid Mech*., **476**, 191-223.

Prandtl, L., 1925, The Magnus effect and wind-powered ships, *Naturwissenschaften*, **13**, 1787-1806.

Reid, E. G., 1924, Tests of rotating cylinders, NACA TN 209.

Salter, T., Sortino, G. and Latham, J., 2008, Sea-going hardware for the cloud-albedo method of reversing global warming, *Phil Trans Roy Soc*., **3666A**, 3989-4006.

Stojkovic, D., Breuer, M. and Durst, F., 2002, Effects of high rotation on the laminar flow around a circular cylinder, *Phys. Fluids*, **14**, 3160-3178.

Thom, A., 1934, Effects of discs on the air forces on a rotating cylinder, *Aero. Res. Counc.* R&M 1623.

Yap, C. R., 1987, *Turbulent heat and momentum transfer in recirculating and impinging flows*, PhD Thesis, Faculty of Technology, University of Manchester.

Zacharos, A., 2010, *The use of unsteady RANS in the computation of 3-dimensiional flow in rotating cavities*, PhD Thesis, School of MACE, University of Manchester.